

# Oligopeptide-Mediated Acceleration of Amyloid Fibril Formation of Amyloid $\beta$ ( $A\beta$ ) and $\alpha$ -Synuclein Fragment Peptide (NAC)

YOSHIHIRO KURODA,\* YOSHITAKA MAEDA, HIROFUMI HANAOKA, KAZUHIDE MIYAMOTO  
and TERUMICHI NAKAGAWA

Graduate School of Pharmaceutical Sciences, Kyoto University, Kyoto, 606-8501, Japan

Received 24 February 2003

Revised 7 April 2003

**Abstract:** The effects of oligopeptides on the secondary structures of  $A\beta$  and NAC, a fragment of  $\alpha$ -synuclein protein, were studied by circular dichroism (CD) spectra. The effects of oligopeptides on the amyloid fibril formation were also studied by fluorescence spectra due to thioflavine-T. The oligopeptides were composed of a fragment of  $A\beta$  or NAC and were interposed by acidic or basic amino acid residues. The peptide, Ac-ELVFFAKK-NH<sub>2</sub>, which involved a fragment Leu-Val-Phe-Phe-Ala at  $A\beta$ (17–21), had no effect on the secondary structures of  $A\beta$ (1–28) in 60% or 90% trifluoroethanol (TFE) solutions at both pH 3.2 and pH 7.2. However, it showed pronounced effects on the secondary structure of  $A\beta$ (1–28) at pH 5.4. The Ac-ELVFFAKK-NH<sub>2</sub> reduced the  $\alpha$ -helical content, while it increased the  $\beta$ -sheet content of  $A\beta$ (1–28). In phosphate buffer solutions at pH 7.0, Ac-ELVFFAKK-NH<sub>2</sub> had little effect on the secondary structures of  $A\beta$ (1–28). However, it accelerated amyloid fibril formation when monitored by fluorescence spectra due to thioflavine-T. On the other hand, LPFFD, a peptide known as a  $\beta$ -sheet breaker, caused neither an appreciable extent of change in the secondary structure nor amyloid fibril formation in the same buffer solution. The peptide, Ac-ETVK-NH<sub>2</sub>, which involved a fragment Thr-Val at NAC(21–22), had no effect on the secondary structure of NAC in 90% TFE and in isotonic phosphate buffer. However, Ac-ETVK-NH<sub>2</sub> in water with small amounts of NaN<sub>3</sub> and hexafluoroisopropanol greatly increased the  $\beta$ -sheet content of NAC after standing the solution for more than 1 week. Interestingly, in this solution, Ac-ETVK-NH<sub>2</sub> accelerated the fibril formation of NAC. It was concluded that an oligopeptide that involves a fragment of amyloidogenic proteins could be a trigger for the formation of amyloid plaques of the proteins even when it had little effect on the secondary structures of the proteins as monitored by CD spectra for a short incubation time. Copyright © 2003 European Peptide Society and John Wiley & Sons, Ltd.

**Keywords:** Alzheimer's disease; amyloid  $\beta$ ; amyloid fibril; circular dichroism (CD); fluorescence spectra; NAC; oligopeptide; Parkinson's disease;  $\alpha$ -synuclein; thioflavine-T

## INTRODUCTION

Amyloid fibrils formed by amyloidogenic peptides or a protein such as amyloid-beta peptide ( $A\beta$ ), NAC [1], or its precursor protein,  $\alpha$ -synuclein (NACP) [2], are considered to be toxic to neurons. They appear to cause, for example, Alzheimer's disease

[3–5] and Parkinson's disease [5]. The amyloid fibrils are formed by conformational changes from  $\alpha$ -helices to  $\beta$ -sheets [6]. Accordingly, one strategy to overcome the disease would be to find a drug that could stabilize the  $\alpha$ -helical conformations [7] and/or destabilize the  $\beta$ -sheet conformations [8–10] of the amyloidogenic protein. The drug might inhibit the formation of amyloid fibrils [11,12]. Previously, following this strategy, some oligopeptides were proposed that might inhibit amyloid fibril formation

\*Correspondence to: Dr Yoshihiro Kuroda, Graduate School of Pharmaceutical Sciences, Kyoto University, Kyoto 606-8501, Japan; e-mail: yokuroda@pharm.kyoto-u.ac.jp

of prion protein by stabilizing its  $\alpha$ -helices [13]. The oligopeptides are composed of hydrophobic amino acids that include a fragment of the prion protein interposed by acidic or basic amino acid residues. The fragment of the parent protein that involves the hydrophobic amino acids may work as a self-recognition motif [12], while the *N*- and *C*-terminal acidic or basic amino acids may promote salt bridge formation with the basic or acidic amino acids situated before and after the fragment in the amino acid sequence [13,14]. Presently, the effects of oligopeptides constructed likewise from the amino acid sequences of  $A\beta$  and NAC were investigated, on the secondary structures and amyloid fibril formation of these peptides. In contrast to the prion protein peptide, no oligopeptide was found that could stabilize the  $\alpha$ -helical conformation of  $A\beta$  or NAC. On the contrary, some of the oligopeptides greatly accelerated amyloid fibril formation when monitored by fluorescence spectra due to thioflavine-T.

## MATERIALS AND METHODS

### Materials

Amyloid  $\beta$  (1–40) peptide,  $A\beta$ (1–40), was purchased from the Peptide Institute Inc. (Osaka, Japan). NAC was purchased from Bachem AG (Bubendorf, Switzerland). Amyloid  $\beta$  (1–28) peptide,  $A\beta$ (1–28) and all oligopeptides were synthesized automatically by the solid-phase method using Fmoc chemistry on an Applied Biosystems peptide synthesizer, model 433A. After cleavage with trifluoroacetic acid (TFA), the peptides were purified by reverse-phase HPLC on a  $C_{18}$  column with linear gradients of acetonitrile/water with 0.1% TFA. They were characterized by ion spray mass spectrometry.  $A\beta$ (1–28): calcd 3260.53 (monoisotope), 3262.51 (av.), *m/z* found 1632.5 ( $MH^{2+}$ ); KFRHK, Ac-KFRHK-NH<sub>2</sub>: calcd 755.46 (monoisotope), 755.92 (av.), *m/z* found 756.5 ( $MH^+$ ); KSGYK, Ac-KSGYK-NH<sub>2</sub>: calcd 622.34 (monoisotope), 622.72 (av.), *m/z* found 624.0 ( $MH^+$ ); KVHHQE, Ac-KVHHQE-NH<sub>2</sub>: calcd 817.42 (monoisotope), 817.91 (av.), *m/z* found 819.0 ( $MH^+$ ); EVHHQK, Ac-EVHHQK-NH<sub>2</sub>: calcd 817.42 (monoisotope), 817.91 (av.), *m/z* found 819.0 ( $MH^+$ ); ELVFFAKK, Ac-ELVFFAKK-NH<sub>2</sub>: calcd 1021.60 (monoisotope), 1022.26 (av.), *m/z* found 1022.5 ( $MH^+$ ); KLVFFAED, Ac-KLVFFAED-NH<sub>2</sub>: calcd 1008.53 (monoisotope), 1009.17 (av.),

*m/z* found 1010.0 ( $MH^+$ ); KKVGSNE, Ac-KKVGSNE-NH<sub>2</sub>: calcd 801.43 (monoisotope), 801.90 (av.), *m/z* found 802.5 ( $MH^+$ ); EDVGSNK, Ac-EDVGSNK-NH<sub>2</sub>: calcd 788.37 (monoisotope), 788.81 (av.), *m/z* found 789.5 ( $MH^+$ ); LPFFD, LPFFD-OH: calcd 637.31 (monoisotope), 637.74 (av.), *m/z* found 638.0 ( $MH^+$ ); ETVK, Ac-ETVK-NH<sub>2</sub>: calcd 516.29 (monoisotope), 516.60 (av.), *m/z* found 517.0 ( $MH^+$ ); KTVE, Ac-KTVE-NH<sub>2</sub>: calcd 516.29 (monoisotope), 516.60 (av.), *m/z* found 517.0 ( $MH^+$ ).

### Circular Dichroism (CD) Spectra

$A\beta$ (1–28),  $A\beta$ (1–40), NAC, oligopeptides or a mixture of  $A\beta$  or NAC and oligopeptides were dissolved in 60% trifluoroethanol (TFE)–40% H<sub>2</sub>O, 90%TFE–10%H<sub>2</sub>O or in isotonic (305 mOsm, 115 mM) phosphate buffers at concentrations of 30–50  $\mu$ M. The pH was adjusted to the desired value with a pH meter by adding a small amount of HCl or NaOH. CD spectra (190–250 nm) were obtained on a Jasco model J-720 or model J-820 spectropolarimeter at room temperature with a 0.5 mm pathlength quartz cell. The vertical scale of the CD spectra was expressed as a mean residue ellipticity in units of deg cm<sup>2</sup>/dmol. In a mixed system due to  $A\beta$  or NAC and oligopeptides, the mean residue was considered to be the sum of the residue numbers of  $A\beta$  or NAC and oligopeptides. The helicity ( $\alpha$ ) was determined from the mean residue ellipticity [ $\theta$ ] at 222 nm according to the relation  $\alpha = ([\theta]_{222} + 2000) \times 100 / -30\,000$  (%) [15]. The percentages of each secondary structure were analysed by using CONTIN/LL within the CDPro software package [16,17]; the fraction of turns was included in the percentage of random-coils for convenience.

### Fluorometric Determination of Amyloid Fibrils

The quantity of amyloid present was monitored by the change in the fluorescence of thioflavine-T (ThT) associated with its binding to fibrils [18].  $A\beta$ (1–28) or a mixture of  $A\beta$ (1–28) and oligopeptides were dissolved in an isotonic (305 mOsm, 115 mM) phosphate buffer, pH 7.0 at a concentration of 100  $\mu$ M and were incubated at 37 °C for 30 min, 3 h, 6 h, 12 h, 30 h or 60 h. After the incubation period, ThT (2  $\mu$ M) was added and the fluorescence was measured at an excitation wavelength of 435 nm and an emission wavelength of 485 nm with a Shimadzu model RF-5300PC spectrofluorometer. The quantity of amyloid present in NAC was

monitored as in the case of A $\beta$ (1–28) except that the solvents used were pure water with 0.025% NaN<sub>3</sub> and 1% hexafluoroisopropanol (HFIP) at pH 7.0 to facilitate amyloid fibril formation for NAC [19].

## RESULTS

### Effects of Oligopeptides on the Secondary Structures of A $\beta$ (1–28) and A $\beta$ (1–40) in TFE Solutions

Figure 1A shows the amino acid sequence of A $\beta$  and oligopeptides chosen by dissecting fragments according to the amino acid sequences of A $\beta$ . The fragments that involved hydrophobic amino acid(s) were interposed by relevant acidic or basic amino acid residues to promote salt bridge formation with the basic or acidic amino acids of A $\beta$ . According to Barrow *et al.*, the  $\alpha$ -helical structures of A $\beta$  peptides are favoured at pH 1–4 and pH 7–10, while the  $\beta$ -sheets are favoured at pH 4–7 in 60% TFE solutions [20]. Figure 2A and B shows the CD spectra of A $\beta$ (1–28) and the mixture of A $\beta$ (1–28) and various kinds of oligopeptides in 60% TFE solutions at pH 3.2 and pH 7.2, respectively. As seen in these spectra, the oligopeptides had no effect on the secondary structure of A $\beta$ (1–28). Similar observations were tried in 90% TFE solutions, expecting a stabilization of the salt bridges with increasing hydrophobicity of the solution. However, as shown in Figure 2C and D, the oligopeptides had no effect on the secondary structure of A $\beta$ (1–28).

Figure 3A shows the time-dependent changes in the CD spectra of A $\beta$ (1–28) in 60% TFE solution at pH 5.4. At pH 5.4, A $\beta$ (1–28) was

favoured by  $\beta$ -sheets as reflected in the secondary structure analysis by CONTIN/LL (Figure 3B). For the A $\beta$ (1–28) in 60% TFE solutions at pH 5.4, various kinds of oligopeptides including LPFFD were added. It was found that ELVFFAKK and LPFFD exerted the most prominent effects on the secondary structures of A $\beta$ (1–28) as shown in Figure 4. Figure 4A and C shows the CD spectra for A $\beta$ (1–28) and the oligopeptide (A, ELVFFAKK; C, LPFFD) mixed solutions, while Figure 4B and D shows the sum of the CD spectra of the A $\beta$ (1–28) and the oligopeptide (B, ELVFFAKK; D, LPFFD) observed separately. By comparing the CD spectra between Figure 4A and 4B, it was found that ELVFFAKK reduced the negative ellipticity at 207 nm while it increased the negative ellipticity at 217 nm. These results indicate that ELVFFAKK reduced the  $\alpha$ -helical content and increased the  $\beta$ -sheet content of the solution. On the other hand, in the case of LPFFD, the negative ellipticity at 217 nm reduced time-dependently. This result indicates that LPFFD decreased the  $\beta$ -sheet content of the solution, as expected from its nature as a  $\beta$ -sheet breaker [9]. Figure 5 shows the CD spectra of A $\beta$ (1–40) and ELVFFAKK in 60% TFE solutions at pH 5.4. Figure 5A shows the CD spectra observed within 30 min after preparing the sample solutions, while Figure 5B shows the CD spectra observed 1 week after preparing the sample solutions. The bold lines were the CD spectra of A $\beta$ (1–40) and the oligopeptide mixed solutions, while the thin lines were the sum of the CD spectra of A $\beta$ (1–40) and the oligopeptide observed separately. Interestingly, the difference in the spectral shapes shown by the bold line and the thin line increased for the solution observed 1 week later (Figure 5B), implying

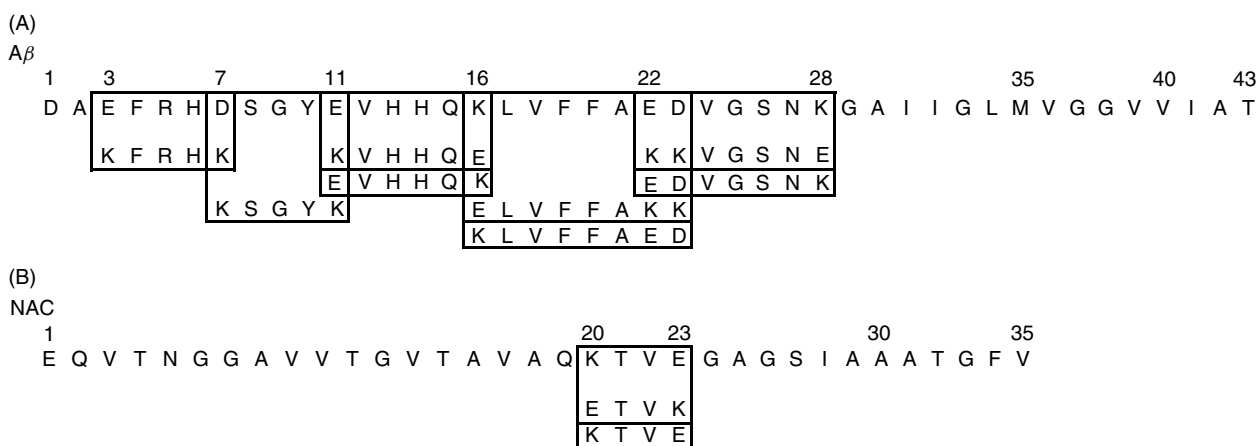


Figure 1 Amino acid sequences of (A) A $\beta$  and (B) NAC. The oligopeptides chosen are shown under each amino acid sequence.

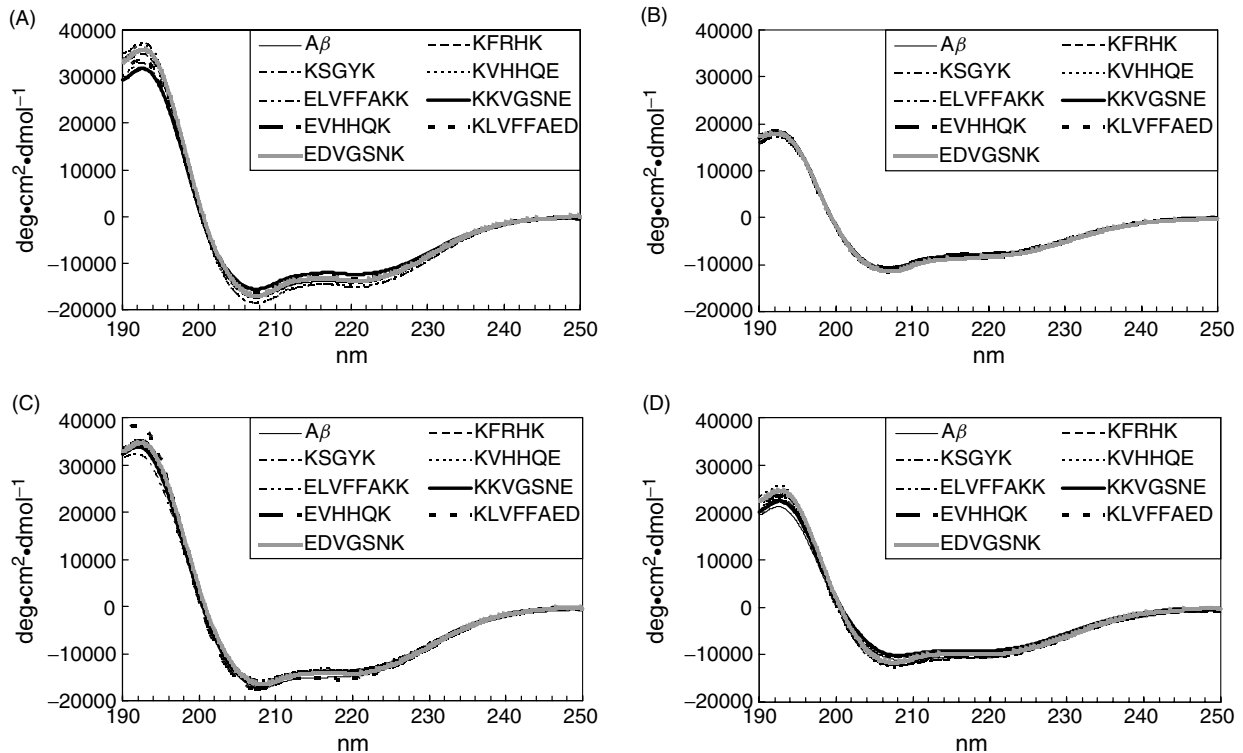


Figure 2 CD spectra of  $A\beta(1-28)$  with various kinds of oligopeptides in (A) and (B), 60% TFE and in (C) and (D), 90% TFE solutions. (A) and (C), pH 3.2. (B) and (D), pH 7.2. The concentrations of all of the peptides were 30  $\mu\text{M}$ .

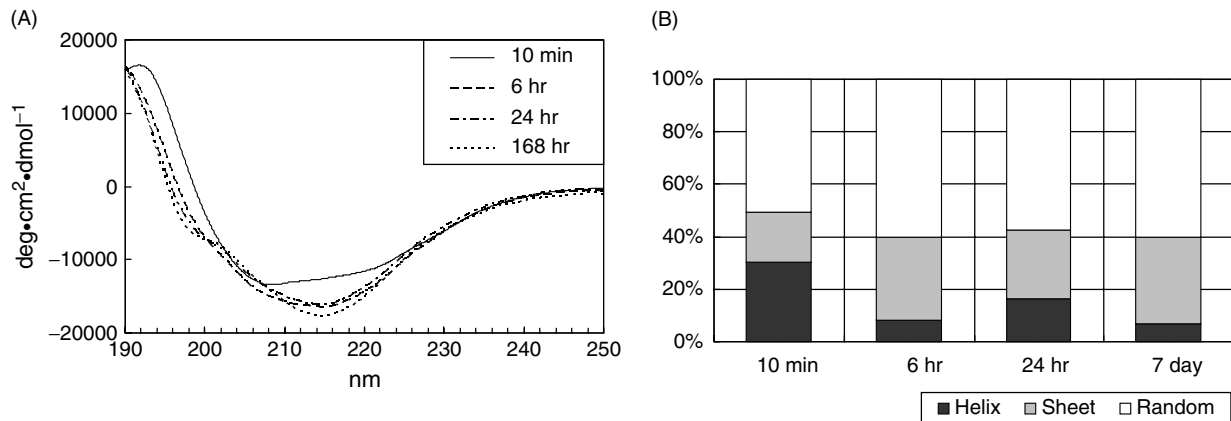


Figure 3 (A) Time-dependent CD spectra of  $A\beta(1-28)$  in 60% TFE solutions at pH 5.4. (B) The secondary structure analysis for the CD spectra shown in (A). The concentration of  $A\beta(1-28)$  was 30  $\mu\text{M}$ .

that ELVFFAKK changed the secondary structure of  $A\beta(1-40)$  to a certain extent. However, the extent appeared to be small compared with the case of  $A\beta(1-28)$  which was suggested from the spectral difference between Figure 4A and 4B. This difference in the action of ELVFFAKK on  $A\beta$  may be due to the difference in the secondary structures between  $A\beta(1-28)$  and  $A\beta(1-40)$ .

#### Effects of ELVFFAKK and LPFFD on the Secondary Structures and on the Fluorescence by Thioflavine-T (ThT) of $A\beta(1-28)$ in Isotonic Phosphate Buffer Solutions at pH 7.0–7.4

Figure 6A and B shows, respectively, the CD spectra of  $A\beta(1-28)$  and the mixture of  $A\beta(1-28)$  and ELVFFAKK in phosphate buffer solutions at pH 7.4. As shown in Figure 6A,  $A\beta(1-28)$  solution showed no

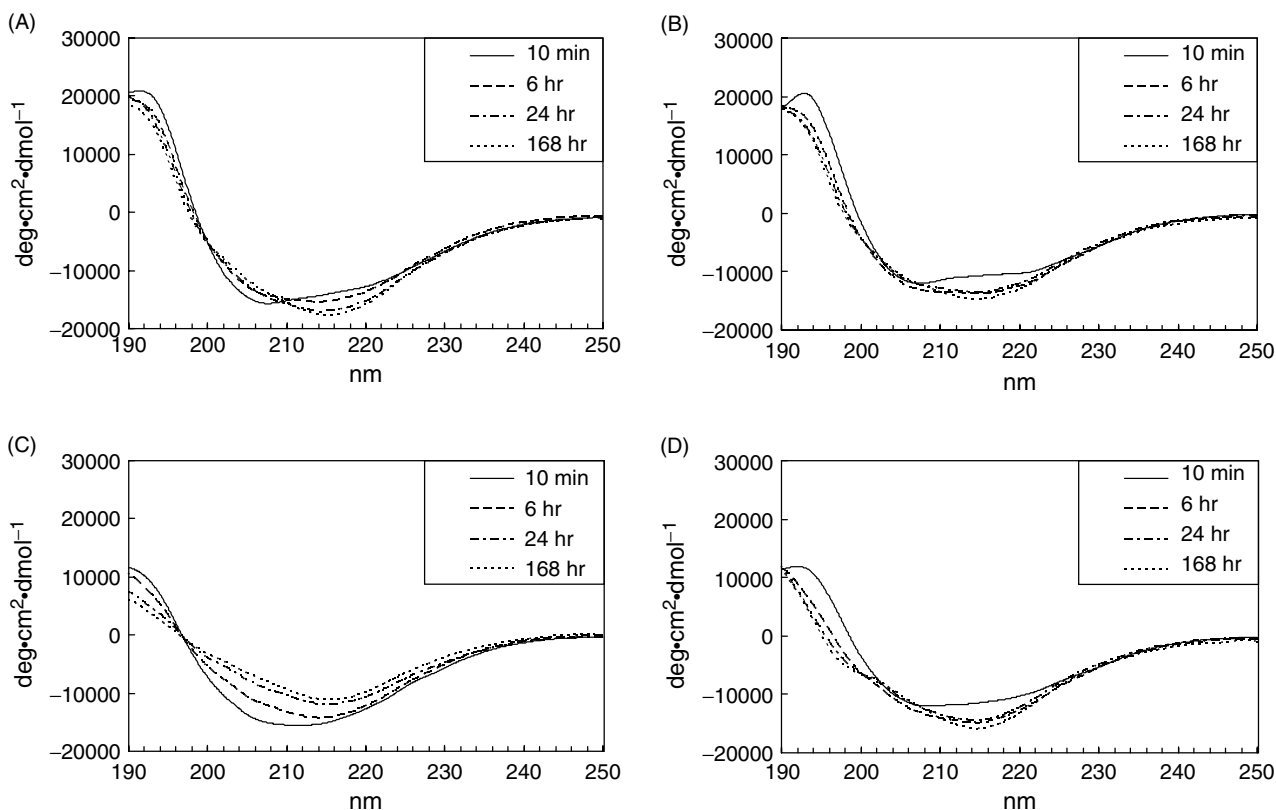


Figure 4 (A) and (C), CD spectra of  $A\beta(1-28)$  with ELVFFAKK and LPFFD, respectively, in 60% TFE solutions at pH 5.4. (B) and (D), sum of the CD spectra of  $A\beta(1-28)$  and the oligopeptide (B, ELVFFAKK; D, LPFFD) solutions observed separately. The concentration of each peptide was  $30 \mu\text{M}$ .

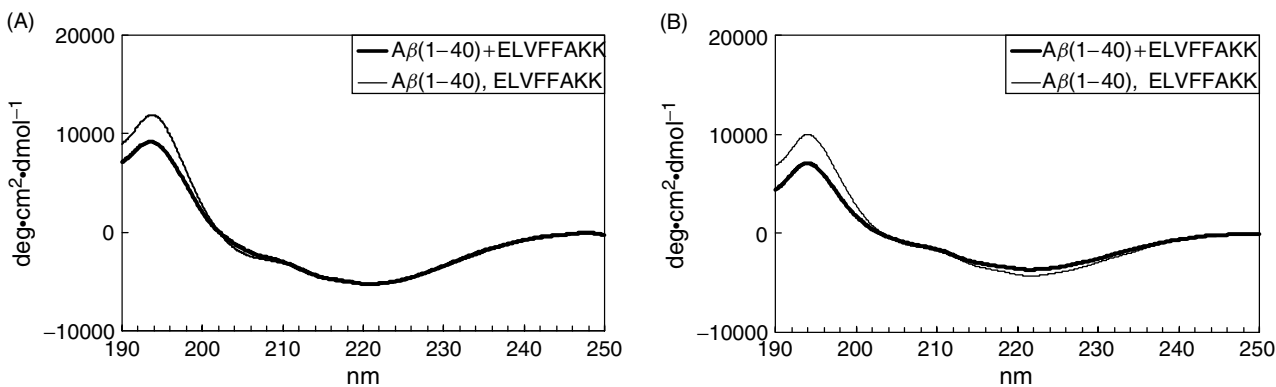


Figure 5 CD spectra of  $A\beta(1-40)$  and ELVFFAKK in 60% TFE at pH 5.4 observed (A) within 30 min and (B) 1 week later after preparing the sample solutions. Bold lines were CD spectra of  $A\beta(1-40)$  and the oligopeptide mixed solutions and thin lines were the sum of the CD spectra of  $A\beta(1-40)$  and the oligopeptide observed separately. The concentration of each peptide was  $30 \mu\text{M}$ .

time-dependent changes in the CD spectra, whereas in Figure 6B,  $A\beta(1-28)$  with ELVFFAKK solution showed changes in the CD spectra on standing the solution for 7 days (168 h). Secondary structure

analysis for the spectra showed that the content of the random-coils decreased by 7%, while that of the  $\beta$ -sheets increased by 10%. Evidently, ELVFFAKK increased the content of the  $\beta$ -sheets as in

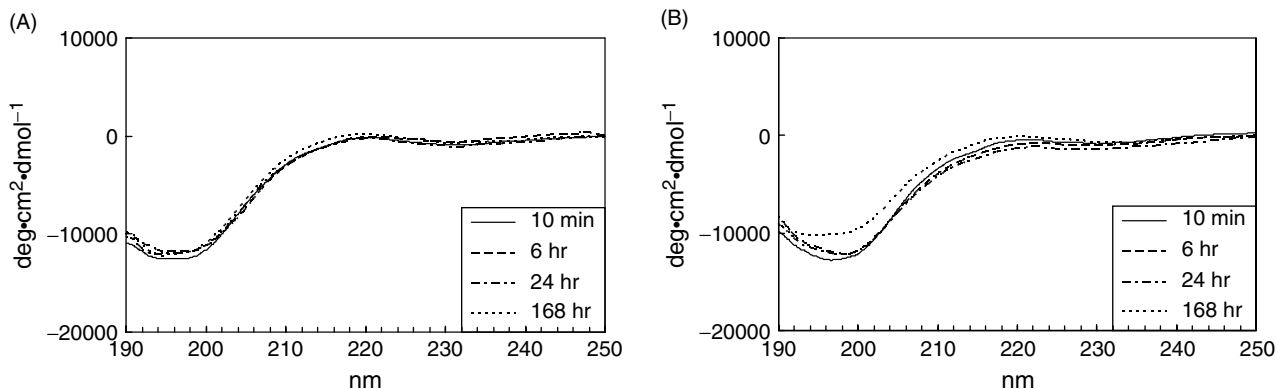


Figure 6 Time-dependent CD spectra of (A)  $A\beta(1-28)$  and (B) the mixture of  $A\beta(1-28)$  and ELVFFAKK in phosphate buffer solutions at pH 7.4. The concentration of each peptide was  $30 \mu\text{M}$ .

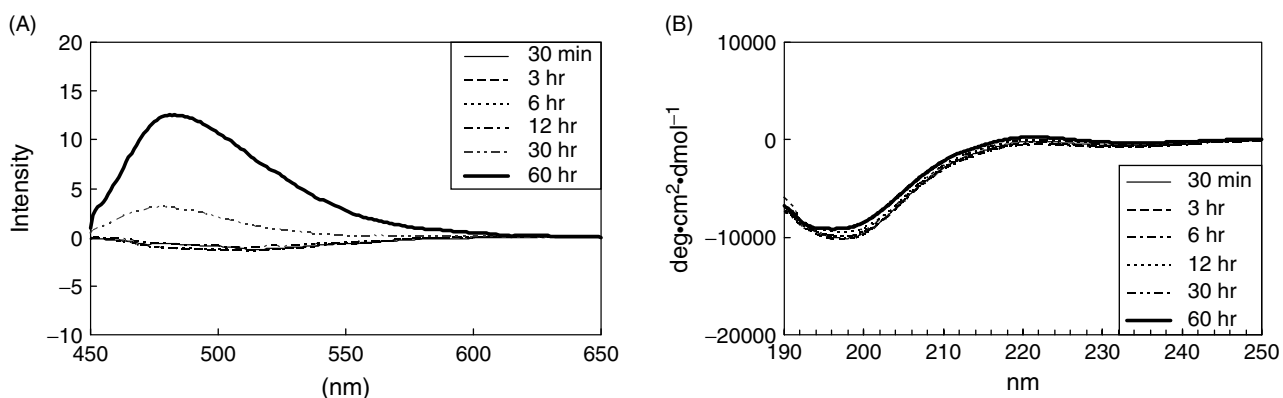


Figure 7 (A) Time-dependent fluorescence spectra of  $A\beta(1-28)$  in phosphate buffer solution at pH 7.0. (B) Time-dependent CD spectra observed at the same incubation times as in the fluorescence experiments. The concentration of  $A\beta(1-28)$  was  $100 \mu\text{M}$  in (A) and  $30 \mu\text{M}$  in (B).

the case of 60% TFE solution at pH 5.4. In order to characterize the increase in the  $\beta$ -sheet content by ELVFFAKK in relation to amyloid fibril formation, the fluorescence spectra due to ThT were determined. Figure 7A and B shows, respectively, the time-dependent fluorescence spectra of  $A\beta(1-28)$  in phosphate buffer solution at pH 7.0 and the corresponding CD spectra observed at the corresponding incubation times as in the fluorescence experiments. Figure 7A shows that the solution including only  $A\beta(1-28)$  slightly produced amyloid fibrils at an incubation time of 30 h or more; however, the corresponding CD spectra at 30 h or more showed no marked changes in the line-shape. Figure 8 shows the time-dependent fluorescence and CD spectra of  $A\beta(1-28)$  and ELVFFAKK (Figure 8A and B) or LPFFD (Figure 8C and D) mixed solutions. Figure 8A

clearly shows that ELVFFAKK increased dramatically the fluorescence intensities due to ThT, showing that amyloid fibrils had already been formed at an incubation time of 12 h. On the other hand, LPFFD had essentially no effect on the fluorescence intensities (Figure 8C). Notably, in both cases, the corresponding CD spectra showed no marked changes in their line-shapes. These results show that the CD spectra which represent overall secondary structures of the solution are insensitive for monitoring the initial stage of amyloid fibril formation. Moreover, the present results show that the oligopeptide involving a fragment of LVFFA greatly accelerated amyloid fibril formation, whereas the oligopeptide LPFFD which consists of the modified amino acid sequence from LVFFA and includes a proline residue dramatically inhibited amyloid fibril formation.

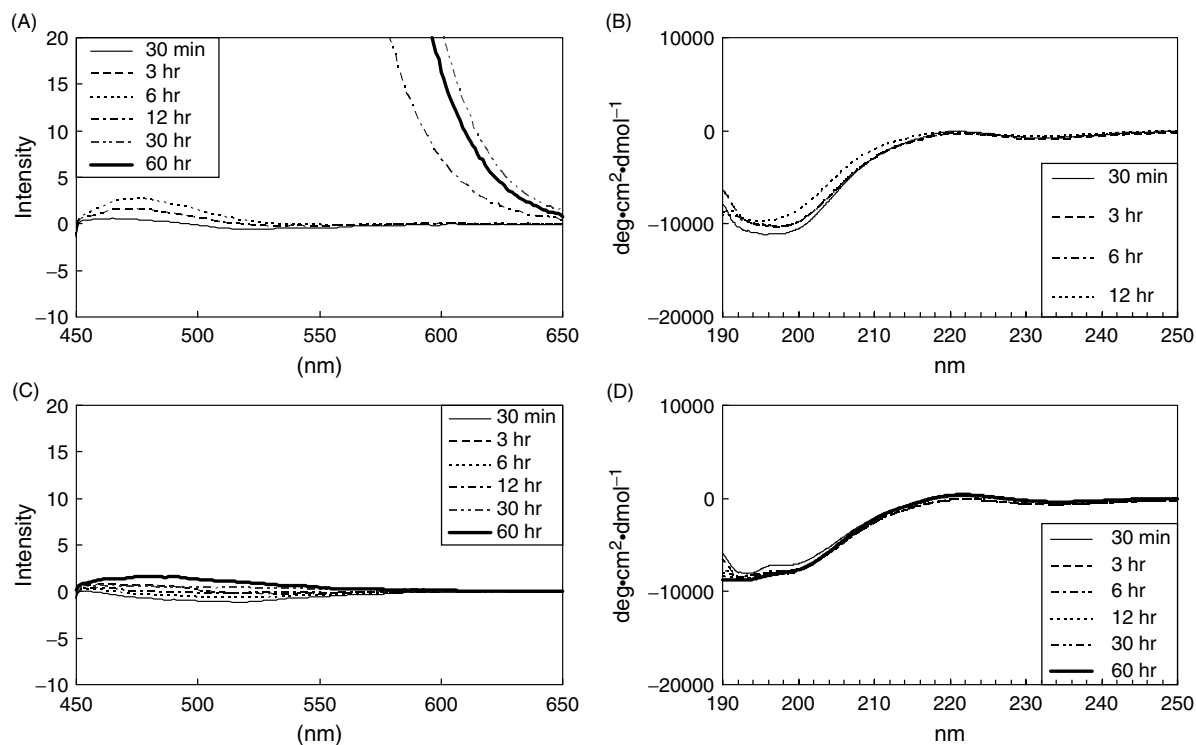


Figure 8 (A) Time-dependent fluorescence spectra of Aβ(1–28) with ELVFFAKK in phosphate buffer solution at pH 7.0. (B) Time-dependent CD spectra observed at the same incubation times as in the fluorescence experiments in (A). (C) Time-dependent fluorescence spectra of Aβ(1–28) with LPFFD in phosphate buffer solution at pH 7.0. (D) Time-dependent CD spectra observed at the same incubation times as in the fluorescence experiments in (C). The concentrations of Aβ(1–28) and ELVFFAKK or LPFFD were 100 μM in (A) and (C) and 30 μM in (B) and (D).

### Effects of Oligopeptides on the Secondary Structures of NAC in 90% TFE and in Isotonic Phosphate Buffer Solutions at pH 7.0

NAC contains only one site that can be considered an oligopeptide, i.e. ETVK or KTVE, according to the strategies used to select the oligopeptide (Figure 1B) [13]. Figure 9A and B shows the CD spectra of NAC and oligopeptides in 90% TFE, whereas Figure 9C and D shows the CD spectra of NAC and oligopeptides in isotonic phosphate buffer solutions. The observed spectral line-shapes clearly show that NAC in 90% TFE assumes  $\alpha$ -helices, whereas NAC in buffer assumes random-coils. The secondary structures of NAC were very little affected by ETVK or KTVE in both 90% TFE and buffer solutions at least within 1 h.

### Time-dependent Effects of ETVK on the Secondary Structures and on the Fluorescence Spectra due to Thioflavine-T (ThT) of NAC in Water with Small Amounts of NaN<sub>3</sub> and HFIP at pH 7.0

Figure 10A shows the time-dependent changes in the CD spectra of NAC in water with small

amounts of NaN<sub>3</sub> and HFIP. This solvent system was chosen to facilitate amyloid fibril formation for NAC [19]. Figure 10A clearly shows that the secondary structure of NAC itself changes from random-coils to  $\beta$ -sheets. Figure 10B shows time-dependent changes in the CD spectra of the mixture of NAC and ETVK in the same solvent system as in Figure 10A. The solid lines show the CD spectra observed within 1 h, whereas the dotted lines show the CD spectra observed 12 days (288 h) later after preparing the sample solutions; bold lines show the CD spectra of NAC and ETVK mixed solutions, while thin lines show the sum of the CD spectra of NAC and ETVK observed separately. As seen from these spectra, the secondary structures of NAC were dramatically changed from random-coils (solid lines) to  $\beta$ -sheets (dotted lines). Moreover, it is evident that ETVK greatly accelerated the conformational change of NAC. This effect of ETVK on the secondary structure of NAC was well reflected in the fluorescence spectra due to ThT. Figure 11 shows the fluorescence spectra of NAC solutions without (Figure 11A) and with ETVK (Figure 11B).

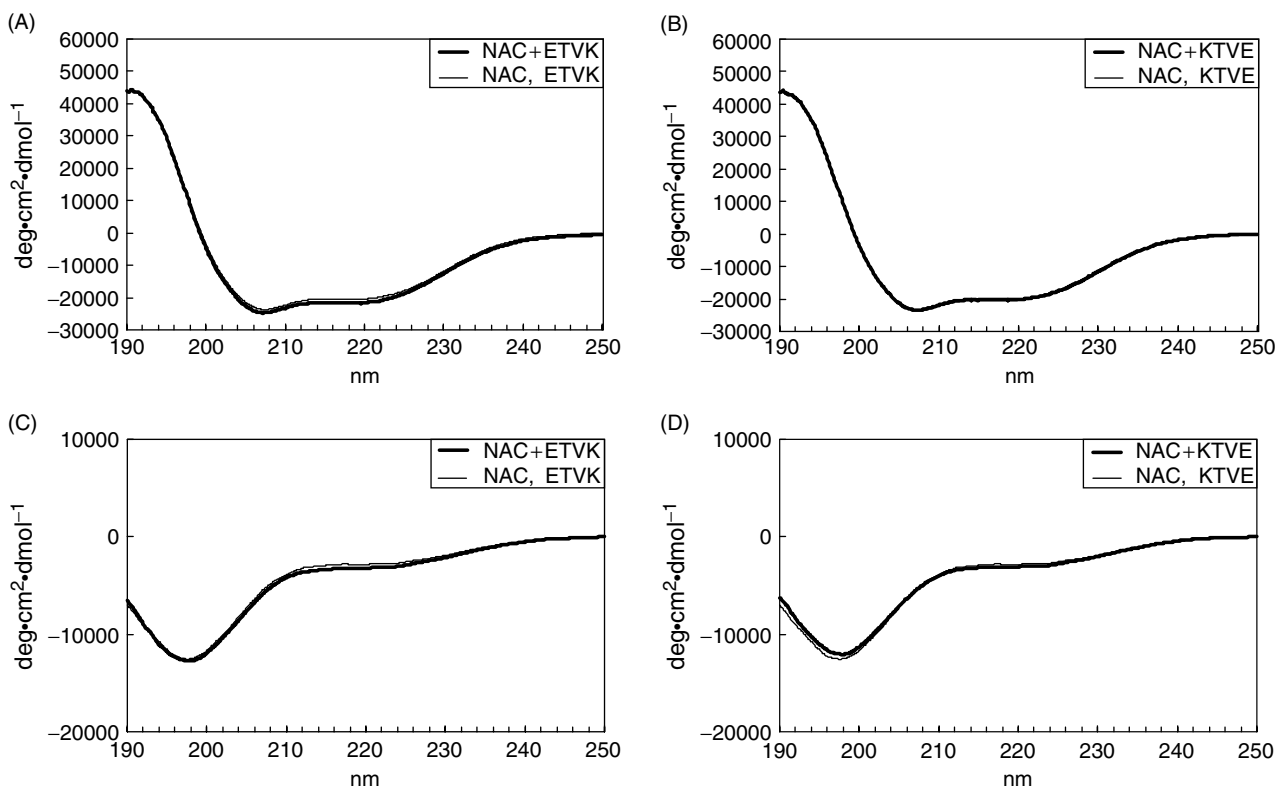


Figure 9 (A) and (B), CD spectra of NAC and oligopeptides in 90% TFE at pH 7.0. (C) and (D), CD spectra of NAC and oligopeptides in isotonic phosphate buffer solutions. The concentration of each peptide was  $50\ \mu\text{M}$ .

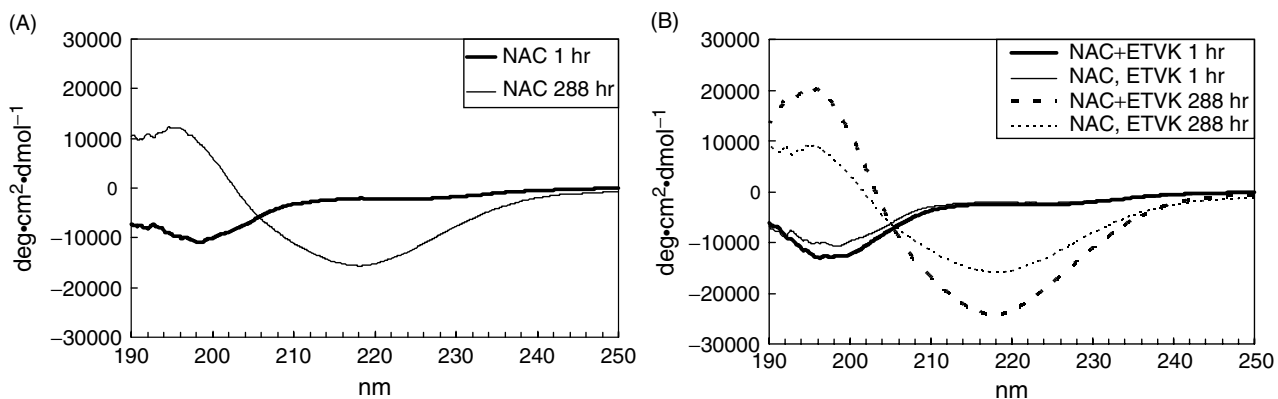


Figure 10 (A) CD spectra of NAC in water with ThT ( $1\ \mu\text{M}$ ) and small amounts of  $\text{NaN}_3$  and HFIP at pH 7.0; bold line, observed within 1 h, thin line, observed 12 days (288 h) later after preparing sample solutions. (B) CD spectra of NAC and ETVK in water with ThT ( $1\ \mu\text{M}$ ) and small amounts of  $\text{NaN}_3$  and HFIP at pH 7.0. Solid lines, observed within 1 h, dotted lines, observed 12 days (288 h) later after preparing sample solutions; bold lines show the CD spectra of NAC and ETVK mixed solutions, while thin lines show the sum of the CD spectra of NAC and ETVK observed separately. The concentration of each peptide was  $30\ \mu\text{M}$ .



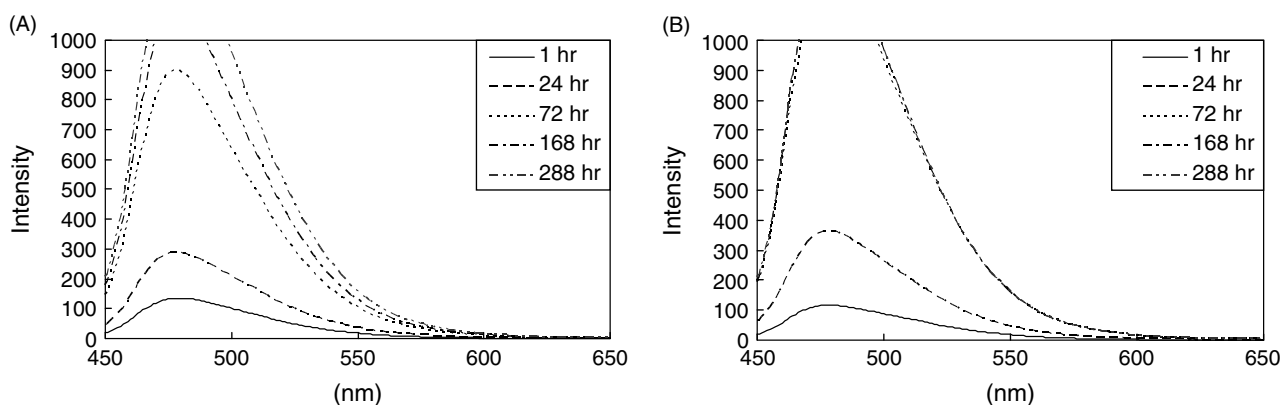


Figure 11 Time-dependent fluorescence spectra of NAC solutions (A) without and (B) with ETVK at pH 7.0. The concentration of each peptide and ThT was 30  $\mu\text{M}$  and 1  $\mu\text{M}$ , respectively.

It is clearly seen that after 24 h or more, the intensities of the fluorescence spectra of NAC with ETVK solutions were much stronger than those of the corresponding pure NAC solutions. These results indicate that the oligopeptide that is made up of only four amino acid residues greatly accelerated amyloid fibril formation.

## DISCUSSION

Taken together the present results show that no  $\alpha$ -helix stabilizing oligopeptides were found for  $A\beta$  and NAC in 60%–90% TFE. This is in contrast to our previous work with a prion protein peptide, in which some oligopeptides were found that could stabilize the  $\alpha$ -helical structure of the prion protein peptide in 80%–90% TFE, but not in phosphate buffer solutions [13]. In the present work, oligopeptides that involved a fragment of  $A\beta$  or NAC accelerated the amyloid fibril formation of  $A\beta(1-28)$  and NAC in phosphate buffer and in water, respectively. In these cases, the secondary structures as revealed by CD spectra at first showed no changes in the CD spectra after a short incubation time, but later they showed an increased  $\beta$ -sheet content on standing the solution for a long time. Thus care is required in handling the peptide or in designing therapeutic agents from the peptide that include a fragment of amyloidogenic proteins. Soto *et al.* showed that LPFFD, which was constructed by modifying the amino acid sequence of  $A\beta(17-21)$ , i.e. LVFFA, can be an effective  $\beta$ -sheet breaker to inhibit  $A\beta(1-42)$  amyloid fibril formation [9,11,12]. The amino acid sequence LVFFA is known to be an important determinant of  $A\beta$  fibrillogenesis [7,20]. Thus the

effectiveness of LPFFD is undoubtedly due to the proline residue [9]. The usefulness of LPFFD as a  $\beta$ -sheet breaker was also confirmed in our present fibrillogenesis experiments with  $A\beta(1-28)$ .

NAC has been found in aggregated fibrils of Alzheimer's patients [1,5]. Its amyloid fibrils are considered to seed the polymerization of  $A\beta$  peptides [21] and thus could be a link between Parkinson's and Alzheimer's diseases [22]. ETVK was found to be a strong promoter for making amyloid fibrils of NAC, implying that ETVK has a high affinity for NAC. A possible explanation for the high affinity of ETVK with NAC may be due to the Val-Thr and Thr-Val motifs in the amino acid sequence of NAC (Figure 1B). These motifs appear four times in the amino acid sequence of NAC and might have served as a self-recognition motif to attract ETVK and NAC to each other. Now, it may be possible to design a  $\beta$ -sheet breaker peptide to inhibit NAC aggregation using ETVK or KTVE as a template as in the case of LPFFD for  $A\beta$ . An oligopeptide that is composed of the amino acid sequence of ETVK or KTVE and a proline residue would become an effective  $\beta$ -sheet breaker for NAC aggregation. The oligopeptide could be a useful lead compound in designing therapeutic agents for Alzheimer's disease as well as for Parkinson's disease. Work to find such an oligopeptide is currently underway.

## REFERENCES

1. Uéda K, Fukushima H, Masliah E, Xia Y, Iwai A, Yoshimoto M, Otero DAC, Kondo J, Ihara Y, Saitoh T. Molecular cloning of cDNA encoding an unrecognized

- component of amyloid in Alzheimer disease. *Proc. Natl. Acad. Sci. USA* 1993; **90**: 11 282–11 286.
2. Uéda K, Saitoh T, Mori H. Tissue-dependent alternative splicing of mRNA for NACP, the precursor of non- $A\beta$  component of Alzheimer's disease amyloid. *Biochem. Biophys. Res. Commun.* 1994; **205**: 1366–1372.
  3. Yoshimoto M, Iwai A, Kang D, Otero DAC, Xia Y, Saitoh T. NACP, the precursor protein of the non-amyloid  $\beta/A4$  protein ( $A\beta$ ) component of Alzheimer disease amyloid, binds  $A\beta$  and stimulates  $A\beta$  aggregation. *Proc. Natl. Acad. Sci. USA* 1995; **92**: 9141–9145.
  4. Jensen PH, Højrup P, Hager H, Nielsen MS, Jacobsen L, Olesen OF, Gliemann J, Jakes R. Binding of  $A\beta$  to  $\alpha$ - and  $\beta$ -synucleins: identification of segments in  $\alpha$ -synuclein/NAC precursor that bind  $A\beta$  and NAC. *Biochem. J.* 1997; **323**: 539–546.
  5. Iwai A. Properties of NACP/ $\alpha$ -synuclein and its role in Alzheimer's disease. *Biochim. Biophys. Acta* 2000; **1502**: 95–109.
  6. Serpell LC. Alzheimer's amyloid fibrils: structure and assembly. *Biochim. Biophys. Acta* 2000; **1502**: 16–30.
  7. Soto C, Castano EM, Frangione B, Inestrosa NC. The  $\alpha$ -helical to  $\beta$ -strand transition in the amino-terminal fragment of the amyloid  $\beta$ -peptide modulates amyloid formation. *J. Biol. Chem.* 1995; **270**: 3063–3067.
  8. Ghanta J, Shen C-L, Kiessling LL, Murphy RM. A strategy for designing inhibitors of  $\beta$ -amyloid toxicity. *J. Biol. Chem.* 1996; **271**: 29 525–29 528.
  9. Soto C, Kindy MS, Baumann M, Frangione B. Inhibition of Alzheimer's amyloidosis by peptides that prevent  $\beta$ -sheet conformation. *Biochem. Biophys. Res. Commun.* 1996; **226**: 672–680.
  10. Pallitto MM, Ghanta J, Heinzelman P, Kiessling LL, Murphy RM. Recognition sequence design for peptidyl modulators of  $\beta$ -amyloid aggregation and toxicity. *Biochemistry* 1999; **38**: 3570–3578.
  11. Soto C. Plaque busters: strategies to inhibit amyloid formation in Alzheimer's disease. *Mol. Med. Today* 1999; **5**: 343–350.
  12. Soto C. Protein misfolding and disease; protein refolding and therapy. *FEBS Lett.* 2001; **498**: 204–207.
  13. Kuroda Y, Maeda Y, Nakagawa T. Oligopeptide-mediated stabilization of the  $\alpha$ -helix of a prion protein peptide. *J. Am. Chem. Soc.* 2000; **122**: 12 596–12 597.
  14. Kuroda Y, Maeda Y, Miyamoto K, Tanaka K, Kanaori K, Otaka A, Fujii N, Nakagawa T.  $^1\text{H-NMR}$  and circular dichroism spectroscopic studies on changes in secondary structures of the sodium channel inactivation gate peptides as caused by the pentapeptide KIFMK. *Biophys. J.* 1999; **77**: 1363–1373.
  15. Wu C-SC, Ikeda K, Yang JT. Ordered conformation of polypeptides and proteins in acidic dodecyl sulfate solution. *Biochemistry* 1981; **20**: 566–570.
  16. Sreerama N, Venyaminov SY, Woody RW. Estimation of protein secondary structure from circular dichroism spectra: inclusion of denatured proteins with native proteins in the analysis. *Anal. Biochem.* 2000; **287**: 243–251.
  17. Sreerama N, Woody RW. Estimation of protein secondary structure from circular dichroism spectra: comparison of CONTIN, SELCON, and CDSSTR methods with an expanded reference set. *Anal. Biochem.* 2000; **287**: 252–260.
  18. LeVine III H. Thioflavine T interaction with synthetic Alzheimer's disease  $\beta$ -amyloid peptides: detection of amyloid aggregation in solution. *Protein Sci.* 1993; **2**: 404–410.
  19. El-Agnaf OMA, Bodles AM, Guthrie DJS, Harriott P, Irvine GB. The  $N$ -terminal region of non- $A\beta$  component of Alzheimer's disease amyloid is responsible for its tendency to assume  $\beta$ -sheet and aggregate to form fibrils. *Eur. J. Biochem.* 1998; **258**: 157–163.
  20. Barrow CJ, Yasuda A, Kenny PTM, Zagorski MG. Solution conformations and aggregational properties of synthetic amyloid  $\beta$ -peptides of Alzheimer's disease. *J. Mol. Biol.* 1992; **225**: 1075–1093.
  21. Han H, Weinreb PH, Lansbury PT. The core of Alzheimer's peptide NAC forms amyloid fibrils which seed and are seeded by  $\beta$ -amyloid: is NAC a common trigger or target in neurodegenerative disease? *Chem. Biol.* 1995; **2**: 163–169.
  22. Heintz N, Zoghbi H.  $\alpha$ -Synuclein — a link between Parkinson and Alzheimer diseases? *Nature Genet.* 1997; **16**: 325–327.